

## PROCESSED MAINSHOCK ACCELEROMETRIC RECORDINGS OF THE 23 OCTOBER 2011 VAN EARTHQUAKE

In collaboration with  
Earthquake Engineering Research Center (EERC)  
Middle East Technical University, Ankara Turkey

Earthquake Department  
Disaster Management and Emergency Presidency (AFAD), Ankara Turkey

### List of Collaborators

Earthquake Engineering Research Center  
(EERC)

M. Abdullah Sandikkaya  
Özkan Kale  
Aida Azari Sisi  
B. Özer Ay  
Sinan Akkar

Disaster Management and Emergency Presidency  
(AFAD)

Ulubey Çeken  
Turgay Kuru  
Aytaç Apak  
Derya Kökbudak  
Eren Tepeuğur  
Hakan Albayrak  
Vedat Öz Saraç  
Selim Sezer  
Cüneyt Şahin

**REPORT NO: METU/EERC 2011-02**

OCTOBER 2011  
ANKARA



**MIDDLE EAST TECHNICAL UNIVERSITY  
EARTHQUAKE ENGINEERING RESEARCH CENTER**

## 1. Introduction

An earthquake occurred on October 23, 2011 at 10:41 (GMT) in Van located in the eastern part of Turkey. The epicentral coordinates are reported as 38.68N – 43.47E by the Earthquake Department of the Disaster and Emergency Management Presidency (AFAD). The depth and magnitude of the earthquake are given as 19.02 km and  $M_L$ 6.7, respectively. The moment tensor solution and the faulting mechanism information are also provided by the same agency. Other national and international seismic agencies also reported the depth, magnitude, epicenter coordinates as well as other relevant source parameters. These are listed in Table 1. Figure 1 shows some of the mapped faults, the epicenter of the mainshock and the distribution of aftershocks that occurred within 2 days after the mainshock. The aftershocks follow SW-NE trend. Figure 2 shows the historical events in the region. Following the mainshock approximately 650 aftershocks occurred in the first 2 days. The magnitude range ( $M_L$ ) of these aftershocks is between 2 and 5.5. The time dependent variation of the aftershocks is given in Figure 3.

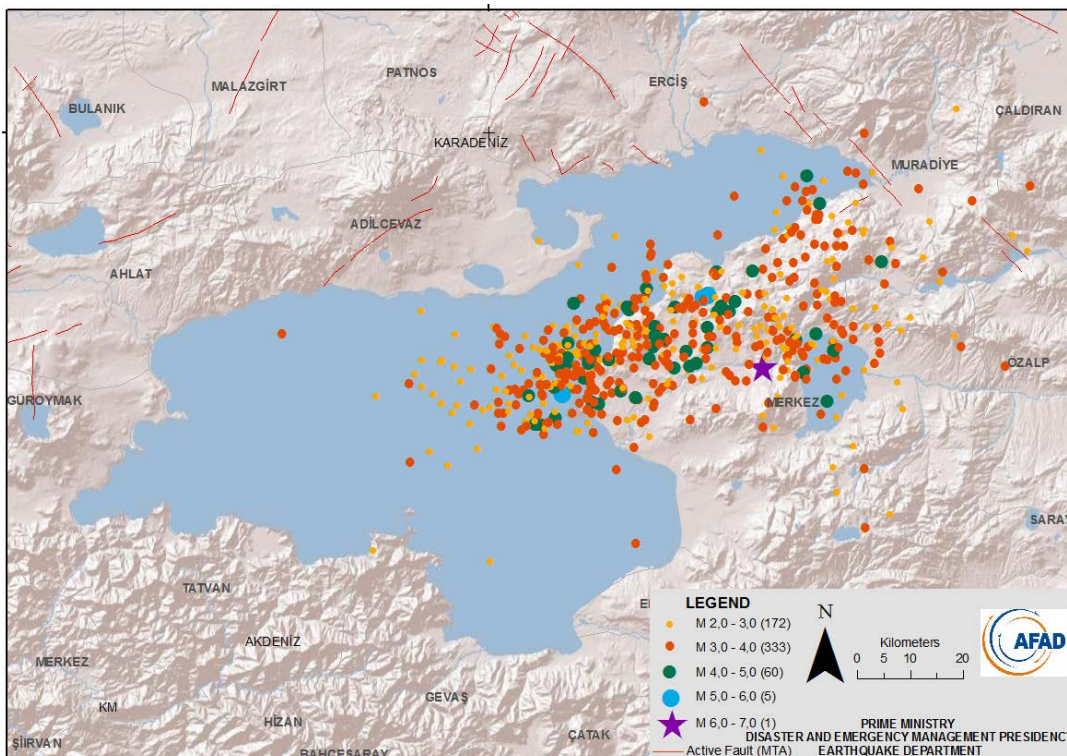


Figure 1. Mapped faults in the vicinity of the earthquake region. The purple star shows the epicentral coordinates of the mainshock. The circles in different sizes show the epicentral coordinates of the aftershocks.

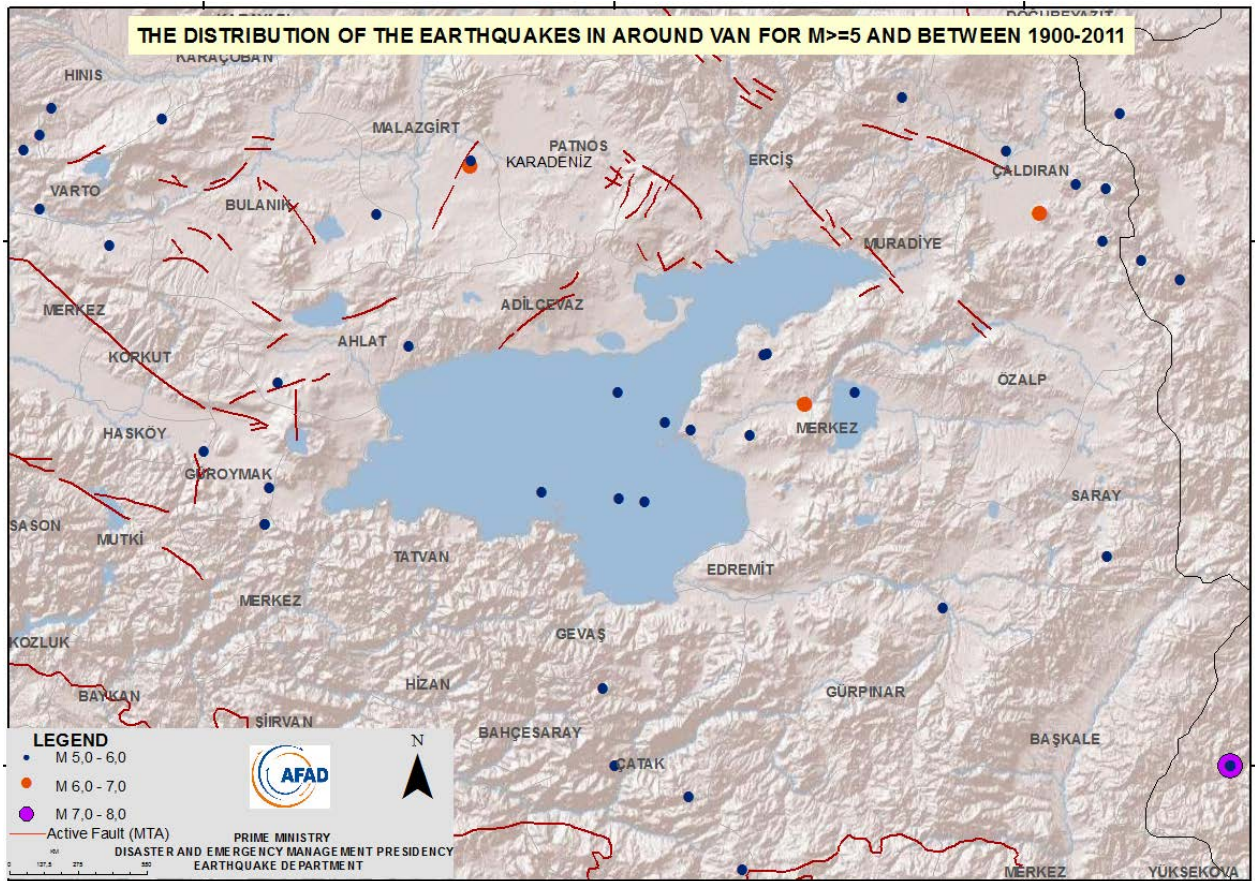


Figure 2. Historic events with M+5 from 1900s to today.

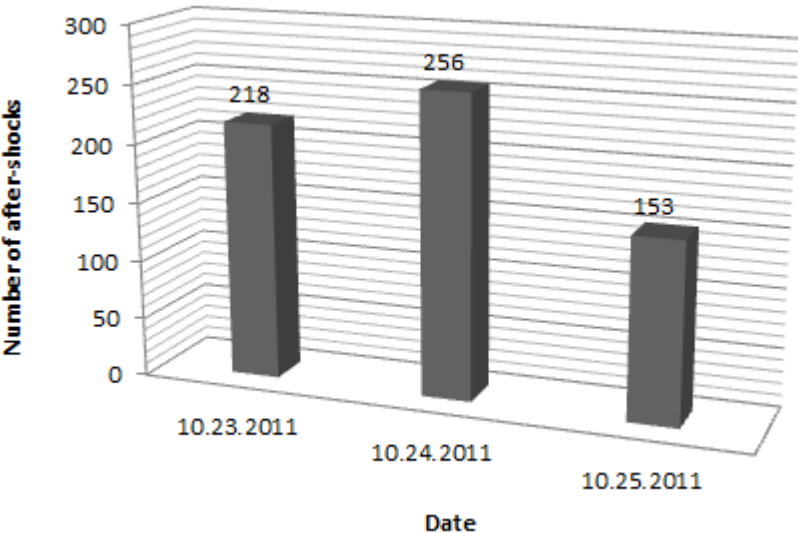


Figure 3. Number of aftershocks in the earthquake region until October 25, 2011.



## 2. Strong-motion data processing:

This major aim of the report is to present the processed accelerometric data recorded during the mainshock. In addition, the comparisons of the observed data with the recently developed ground-motion predictive models are studied. As of October 25, a total of 22 three-component recordings are available through the website <http://kyh.deprem.gov.tr/ftpt.htm> . Figure 4 shows the recording stations with the largest ground acceleration values. The downloaded raw recordings are firstly evaluated by visual inspection to detect the non-standard errors (Douglas, 2003). Then an initial baseline adjustment (mean removal) is applied to the accelerograms. If the accelerogram contains pre-event buffer, the mean of 90% of this pre-event time is removed from the entire record. In the absence of such pre-event segment, the mean of the whole record is removed from the entire accelerogram. Finally, a bi-directional, fourth-order Butterworth filter is applied to band-pass filter the ground-motions. Table 2 summarizes the low-cut and high-cut filter cut-offs determined by the procedure described in Akkar and Bommer (2006), Douglas and Boore (2011) and Akkar et al. (2011). The processing procedure is done by using the USDP software. (This software uses the public-open data processing codes of Dr. David M. Boore at USGS, Menlo Park California). The same table also lists the long-period usable period range of each recording based on the empirical expressions proposed in Akkar and Bommer (2006). Whenever this procedure is inapplicable, usable period is taken as 80% of the low-cut filter period (Abrahamson and Silva, 1997). The processed recordings are disseminated through the web site of METU-EERC. The websites also contains the raw accelerometric data for researchers who want to do their own data processing.

Table 2 shows the coordinates of the stations and  $V_{S30}$  values, if available. This table also lists the source-to-site distance metrics ( $R_{epi}$ ,  $R_{hyp}$ ,  $R_{JB}$  and  $R_{rup}$ ) computed from the information obtained from GCMT<sup>1</sup>. The plane that dips towards North is considered in the distance calculations. This plane is consistent with the alignment of aftershocks given in Figure 1 but it is not still certain. Field observations and refinements in fault-plane solutions will yield the most appropriate fault plane for final distance calculations. The calculation procedure for distance metrics is described by Kakkamonos et al. (2011). The observed values for  $T=0s$ ,  $T=0.2s$ , and  $T=1.0s$  are compared with the estimations of the predictive models developed within the context of the Next Generation Attenuation Models project (i.e., Abrahamson and Silva (2008), Boore and Atkinson (2008), Campbell and Bozorgnia (2008) and Choui and Youngs (2008)), as well the recent Turkish model of Akkar and Cagnan

---

<sup>1</sup> Global Centroid Moment Tensor

(2010). In order to simplify the comparisons, the recordings are converted to  $V_{S30} = 760$  m/s or corresponding rock definitions. Figures 5 and 6 show these comparisons. The response spectra of the recordings whose source-to-site distance metrics are less than 200 km are shown in Figures A1-9.

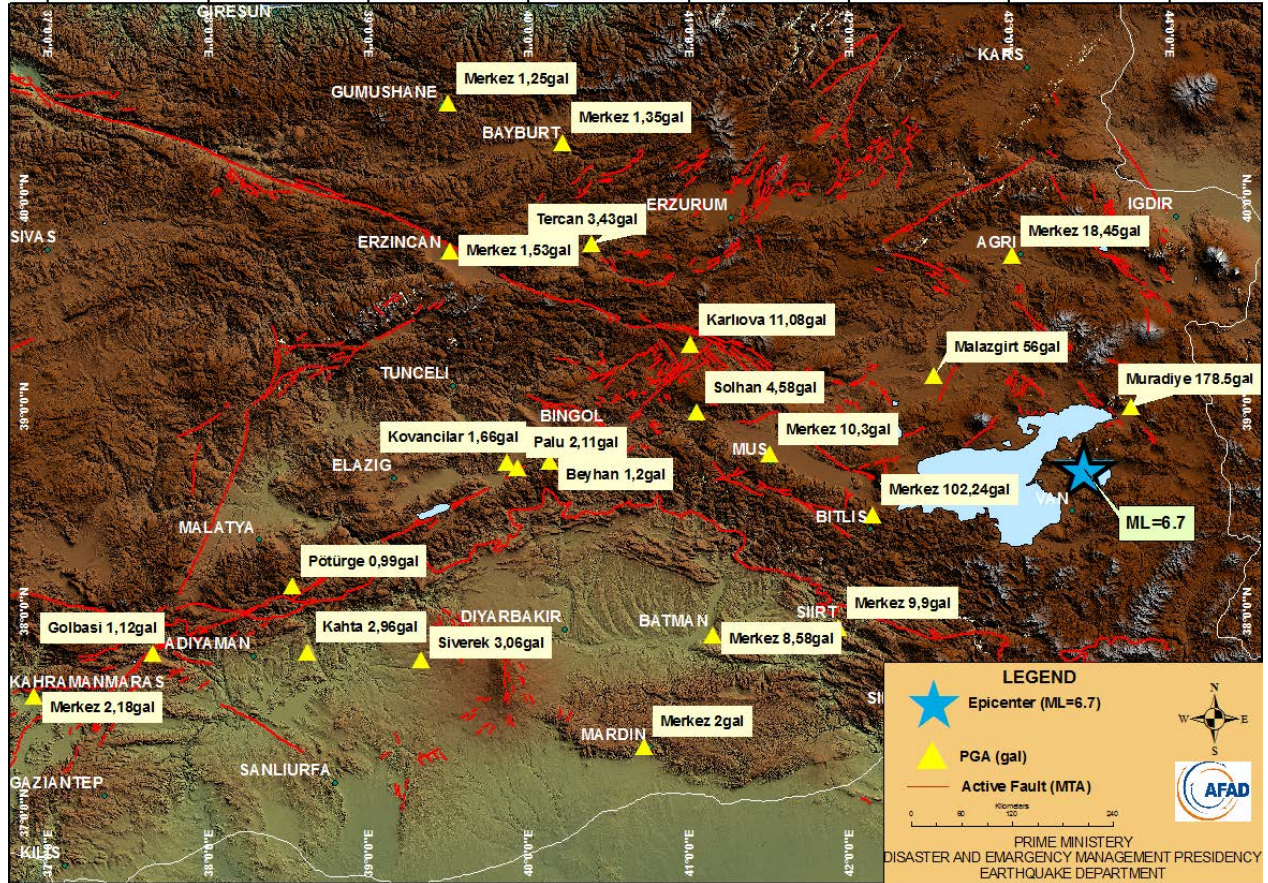


Figure 4. Distribution of strong-motion stations recorded during the mainshock.

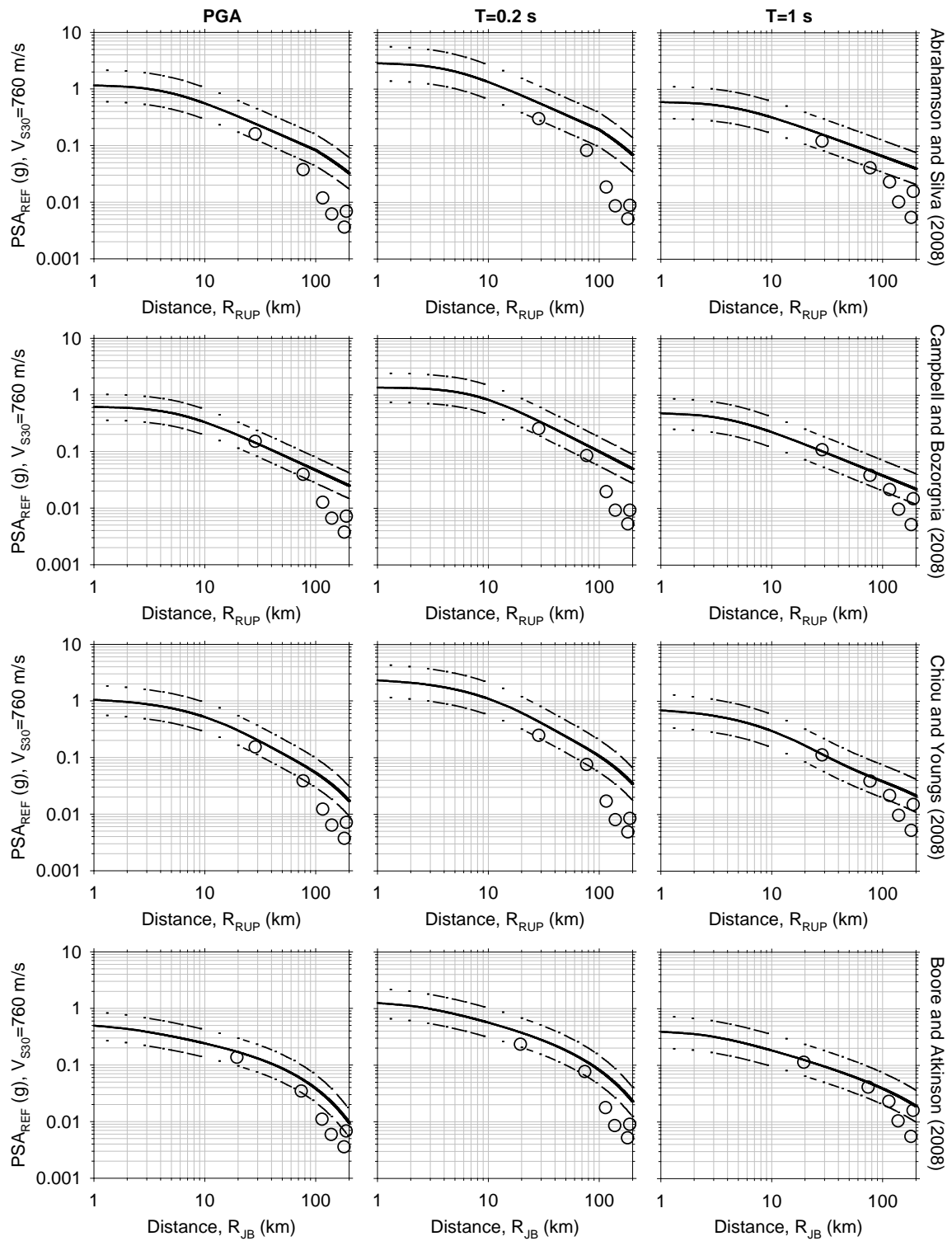


Figure 5. Comparisons of the observed data with NGA predictive models. Left, middle and right columns show the comparative plots for  $T=0 \text{ s}$ ,  $T=0.2 \text{ s}$ , and  $T=1.0 \text{ s}$ , respectively.

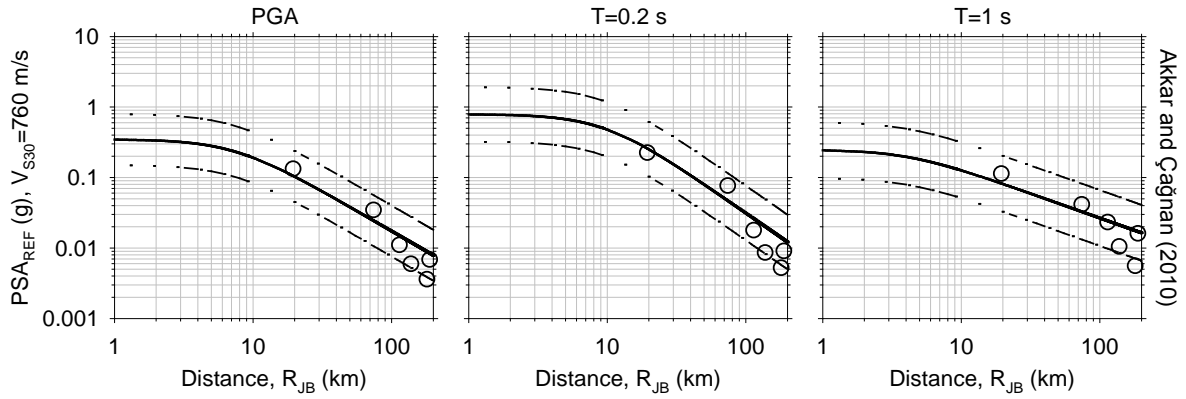


Figure 6. Comparisons of the observed data with Akkar and Çağnan (2010) predictive model. Left, middle and right columns show the comparative plots for  $T=0$  s,  $T=0.2$  s, and  $T=1.0$  s, respectively.

### 3. Information on the Van Earthquake from other national institutions:

Kandilli Observatory and Earthquake Research Institute (<http://www.koeri.boun.edu.tr/>) prepared 2 reports on the 23 October Van earthquake that are posted on the web sites of the Earthquake Engineering Department and National Earthquake Monitoring Center (UDIM). The Geophysical Engineering Department of the Sakarya University (<http://www.ifm.sakarya.edu.tr/>) and the Earthquake Department of the Disaster and Emergency Management Presidency (AFAD) (<http://www.deprem.gov.tr>) also prepared reports on the Van earthquake.

## References

Abrahamson, N.A. and Silva, W.J. (1997). Empirical response spectral attenuation relations for shallow crustal earthquakes, *Seismological Research Letters*, 68: 94-127.

Abrahamson, N.A. and Silva, W. (2008). Summary of the Abrahamson and Silva NGA ground motion relations, *Earthquake Spectra*, 24: 67-98.

Akkar, S. and Bommer, J.J., (2006). " Influence of long-period filter cut-off on elastic spectral displacements," *Earthquake Engineering and Structural Dynamics* , 35(9), 1145-1165.

Akkar, S. and Bommer, J.J.,(2010). Empirical Equations for the Prediction of PGA, PGV and Spectral Accelerations in Europe, the Mediterranean Region and the Middle East, *Manuscript accepted for publication in Seismological Research Letters*, Vol:81, 195-206.

Akkar S. and Cagnan Z. (2010). A local ground motion predictive model for Turkey and its comparison with other regional and global ground-motion models, submitted to Bull. Seism. Soc. Am. for publication.

Akkar, S., Kale, O., Yenier, E. and Bommer J.J., 2011. The high-frequency limit of usable response spectral ordinates from filtered analogue and digital strong-motion accelerograms, *Earthquake Engineering and Structural Dynamics*, DOI: 10.1002/eqe.1095

Boore, D. M. and Atkinson, G. M. (2008). Ground motion prediction equations for the average horizontal component of PGA, PGV, and 5%-damped PSA at spectral periods between 0.01 s and 10.0 s, *Earthquake Spectra*, Vol. 24, No. 1, pp. 99-138.

Boore, D. M., and G. M. Atkinson (2008). Ground motion prediction equations for the average horizontal component of PGA, PGV, and 5%-damped PSA at spectral periods between 0.01 s and 10.0 s. *Earthquake Spectra* 24 (1), 99–138.

Campbell, K. W., and Y. Bozorgnia (2008). NGA ground motion model for the geometric mean horizontal component of PGA, PGV, PGD and 5% damped linear elastic response spectra for periods ranging from 0.01 to 10 s. *Earthquake Spectra* 24 (1), 139–172.



Chiou, B. S.-J, and R. R. Youngs (2008). An NGA model for the average horizontal component of peak ground motion and response spectra. *Earthquake Spectra* 24 (1), 173–215.

Douglas, J., (2003). What is a poor quality strong-motion record?, *Bulletin of Earthquake Engineering*, 1: 141-156.

Douglas, J. and D. M. Boore (2011). High-frequency filtering of strong-motion records, *Bull. Earthquake Engineering*, 9 ,395--409. (862 Kb).[\\_](#)

Kaklamanos, et al (2011). Estimating unknown input parameters when implementing the NGA ground-motion prediction equations in engineering practice. *Earthquake Spectra*.

Table 1. Important seismological features of the earthquake reported by national and international seismological agencies

Agency	Date	Time (GMT)	Epicenter Latitude	Epicenter Longitude	Depth (km)	M <sub>w</sub>	M <sub>b</sub>	M <sub>s</sub>	M <sub>L</sub>	M <sub>0</sub> (dyne.cm)
AFAD	23/10/2011	10:41:00	38.68	43.47	19.02	-	-	-	6.7	-
KOERI	23/10/2011	10:41:21	38.758	43.360	5.0	7.2	-	-	6.6	-
GCMT	23/10/2011	10:41:30.6	38.67	43.42	15.4	7.1	-	7.2	-	6.4e+26
USGS	23/10/2011	10:41:44.5	38.710	43.446	16	7.3	-	-	-	9.9e+26
GFZ	23/10/2011	10:41:22	38.674	43.581	15	7.1	-	-	-	4.7e+26
EMSC	23/10/2011	10:41:22	38.86	43.48	10	7.2	-	-	-	-
INGV	23/10/2011	10:41:00	38.86	43.48	10	7.3	-	-	-	-
GeoAzur	23/10/2011	10:41:21	38.627	43.535	16<d<23	7.2	-	-	-	6.86e+26

Agency	T-axes PLG	T-axes AZ	N-axes PLG	N-axes AZ	P-axes PLG	P-axes AZ	1st Plane Strike	1st Plane Dip	1st Plane Slip	2nd Plane Strike	2nd Plane Dip	2nd Plane Slip
AFAD	-	-	-	-	-	-	98	66	88	283	24	95
KOERI	-	-	-	-	-	-	-	-	-	-	-	-
GCMT	-	-	-	-	-	-	248	36	60	104	60	110
USGS	63	344	4	81	26	173	80	71	86	272	19	101
GFZ	81	22	3	272	9	182	94	54	94	268	36	85
EMSC	-	-	-	-	-	-	-	-	-	-	-	-
INGV	-	-	-	-	-	-	-	-	-	-	-	-
GeoAzur	-	-	-	-	-	-	107	44	120	248	53	64

AFAD: Earthquake Department of the Disaster and Emergency Management Presidency

KOERI: Kandilli Observatory and Earthquake Research Institute

GCMT: Global Centroid Moment Tensor

USGS: U.S. Geological Survey

GFZ: GFZ German Research Centre for Geosciences

EMSC: European-Mediterranean Seismological Centre

INGV: Istituto Nazionale di Geofisica e Vulcanologia

Table 2. Important properties of the processed records from the main and aftershock events

Record Names	Instrument Type	$f_{lc}$ -NS	$f_{hc}$ -NS	Usable period-NS	$f_{lc}$ -EW	$f_{hc}$ -EW	Usable period-EW	$f_{lc}$ -UD	$f_{hc}$ -UD	Usable period-UD
20111023104043_0401	CMG-5TD	0.07	25	13.86	0.07	25	13.86	0.05	25	19.40
20111023104118_1302	CMG-5TD	0.07	0	11.43	0.04	0	20.00	0.04	0	20.00
20111023104120_4902	SM-2	0.06	20	16.17	0.04	20	24.25	0.04	20	24.25
20111023104120_6503	SM-2	0.06	0	16.17	0.04	0	24.25	0.06	0	16.17
20111023104121_5601	CMG-5TD	0.07	20	11.43	0.07	30	11.43	0.07	20	11.43
20111023104134_7201	CMG-5TD	0.04	20	22.50	0.04	20	22.50	0.04	20	22.50
20111023104136_4901	CMG-5TD	0.05	30	19.40	0.15	25	6.47	0.2	30	4.85
20111023104145_1211	CMG-5TD	0.05	0	18.00	0.05	0	18.00	0.05	0	18.00
20111023104156_1206	CMG-5TD	0.04	15	20.00	0.04	0	20.00	0.15	0	5.33
20111023104201_2407	CMG-5TD	0.07	10	13.86	0.05	10	19.40	0.1	10	9.70
20111023104216_4701	CMG-5TD	0.05	25	16.00	0.05	25	16.00	0.05	25	16.00
20111023104221_2305	CMG-5TD	0.05	25	16.00	0.05	25	16.00	0.05	25	16.00
20111023104225_2307	CMG-5TD	0.05	10	19.40	0.05	10	19.40	0.05	10	19.40
20111023104230_2304	CMG-5TD	0.05	0	16.00	0.05	0	16.00	0.05	12	16.00
20111023104240_6901	CMG-5TD	0.07	15	11.43	0.05	15	16.00	0.03	15	26.67
20111023104245_2401	CMG-5TD	0.05	8	19.40	0.05	8	19.40	0.12	8	8.08
20111023104250_6303	CMG-5TD	0.05	15	16.00	0.15	15	5.33	0.15	15	5.33
20111023104255_2902	CMG-5TD	0.05	10	16.00	0.05	10	16.00	0.05	10	16.00
20111023104259_0205	CMG-5TD	0.05	15	16.00	0.05	15	16.00	0.05	15	16.00
20111023104259_4404	CMG-5TD	0.05	12	16.00	0.05	12	16.00	0.05	12	16.00
20111023104330_0208	CMG-5TD	0.05	0	18.00	0.05	0	18.00	0.05	0	18.00
20111023104356_4609	CMG-5TD	0.05	8	19.40	0.05	8	19.40	0.05	8	19.40

$f_{lc}$ : Low-cut filter frequency  
 $f_{hc}$ : High-cut filter frequency

Table 2 (continued)

Record Names	Processed PGA_NS (cm/s <sup>2</sup> )	Processed PGA_EW (cm/s <sup>2</sup> )	Processed PGA_UD (cm/s <sup>2</sup> )	Processed PGV_NS (cm/s)	Processed PGV_EW (cm/s)	Processed PGV_UD (cm/s)
20111023104043_0401	18.3340	14.8930	7.1538	5.4695	4.6567	3.0112
20111023104118_1302	89.6600	102.2200	35.5050	8.8198	7.7020	4.3281
20111023104120_4902	44.3000	55.7510	25.5240	11.9450	11.0720	5.1036
20111023104120_6503	178.5500	169.4500	79.1540	26.3710	14.5700	6.3005
20111023104121_5601	9.6751	9.1262	6.9456	3.7502	3.9307	2.9103
20111023104134_7201	8.2859	8.6086	3.7461	2.9802	2.1375	2.3158
20111023104136_4901	10.3210	7.0842	4.6643	2.5933	1.6551	0.5940
20111023104145_1211	4.6038	4.1524	2.4256	1.9392	2.8055	1.9035
20111023104156_1206	7.5397	11.0710	4.6441	3.0714	4.1079	1.3032
20111023104201_2407	2.3039	3.3930	1.8567	1.0850	2.1882	1.0939
20111023104216_4701	1.9951	1.9068	1.5813	1.3409	1.1224	1.4939
20111023104221_2305	1.2138	1.1698	1.0251	0.7527	0.9547	0.9557
20111023104225_2307	2.1200	1.6455	1.7097	1.1558	1.0578	1.3156
20111023104230_2304	1.4746	1.6514	1.1966	1.4181	0.9167	1.0151
20111023104240_6901	1.3610	1.1140	1.2751	0.6997	1.1137	1.0997
20111023104245_2401	1.5016	1.2808	0.5902	0.8360	1.1664	0.3388
20111023104250_6303	2.0281	3.0715	1.0962	1.2312	0.7855	0.4372
20111023104255_2902	1.0251	0.8194	1.2424	0.8520	0.7302	0.9593
20111023104259_0205	2.9626	2.7268	1.6428	1.3298	1.1463	1.1390
20111023104259_4404	0.9934	1.0041	0.9555	0.9198	0.5280	0.7213
20111023104330_0208	1.1241	0.7444	0.3588	0.4525	0.3915	0.2489
20111023104356_4609	1.7071	2.1414	0.9439	0.7509	1.1942	0.7627

PGA: Peak ground acceleration

PGV: Peak ground velocity



Table 2 (continued)

Record Names	Station Code	Station Latitude	Station Longitude	$V_{S30}$	$R_{epi}$ (km)	$R_{hyp}$ (km)	$R_{JB}$ (km)	$R_{rup}$ (km)
20111023104043_0401	0401	39.71991	43.01585	295	121.829	122.798	114.013	115.89
20111023104118_1302	1302	38.4744	42.15912	-	111.75	112.806	82.8167	85.3772
20111023104120_4902	4902	39.14394	42.53072	311	93.2635	94.5264	74.2502	77.1012
20111023104120_6503	6503	38.99	43.768	293	46.6346	49.1115	19.5117	28.4929
20111023104121_5601	5601	37.9319	41.9353	-	153.363	154.134	124.482	124.885
20111023104134_7201	7201	37.873	41.15116	450	216.978	217.524	188.866	189.138
20111023104136_4901	4901	38.76111	41.50394	315	166.545	167.255	138.216	139.768
20111023104145_1211	1211	38.96616	41.0504	463	207.912	208.481	180.383	181.575
20111023104156_1206	1206	39.29345	41.00883	-	219.633	220.172	194.073	195.182
20111023104201_2407	2407	39.77663	40.39109	320	288.453	288.864	264.726	265.54
20111023104216_4701	4701	37.363	40.723	-	277.366	277.793	248.533	248.735
20111023104221_2305	2305	38.7426	40.13145	-	285.454	285.869	256.922	257.76
20111023104225_2307	2307	38.69581	39.93198	329	302.758	303.149	274.13	274.916
20111023104230_2304	2304	38.7217	39.86441	-	308.606	308.99	280.026	280.795
20111023104240_6901	6901	40.2623	40.2101	-	327.493	327.854	306.178	306.882
20111023104245_2401	2401	39.74183	39.51152	314	357.194	357.526	331.845	332.495
20111023104250_6303	6303	37.75241	39.3291	-	371.661	371.98	342.914	343.543
20111023104255_2902	2902	40.12439	39.43658	-	378.517	378.83	354.769	355.377
20111023104259_0205	0205	37.79179	38.61573	-	430.79	431.065	401.87	402.406
20111023104259_4404	4404	38.19588	38.87385	-	399.434	399.731	370.429	371.011
20111023104330_0208	0208	37.786629	37.653002	469	513.137	513.368	484.145	484.59
20111023104356_4609	4609	37.57531	36.915	317	581.767	581.971	552.793	553.184

$V_{S30}$ : The mean S-wave velocity of the top 30m of the soil profile

$R_{epi}$ : Epicentral distance

$R_{hyp}$ : Hypocentral distance

$R_{JB}$ : Joyner-Boore distance (the closest distance from site to the vertical projection of the rupture plane)

$R_{rup}$ : Rupture distance (the closest distance from site to the rupture plane)

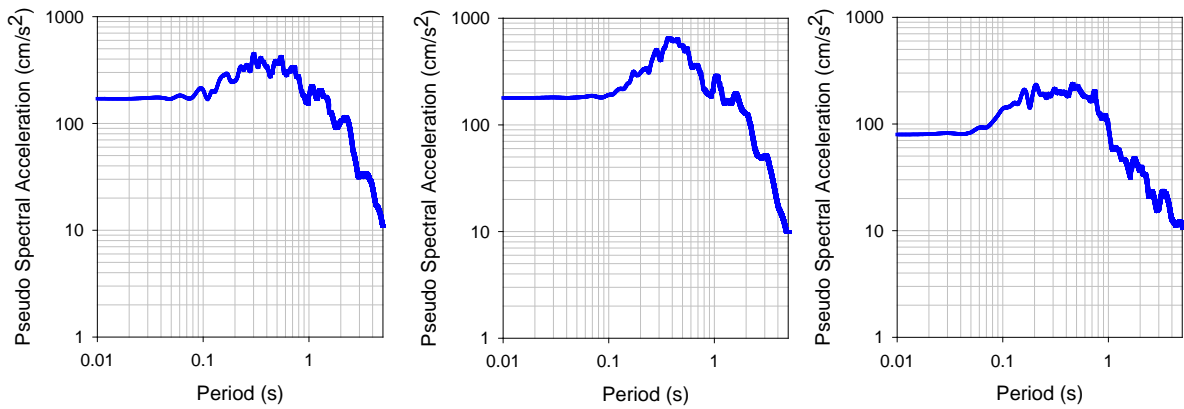


Figure A.1. 5% damped pseudo-spectral accelerations of the processed ground motions recorded at Van-Muradiye (Record Name: 20111023104120\_6503, Station Code: 6503).  
 First column: EW component, second column: NS component and third column: UD component.

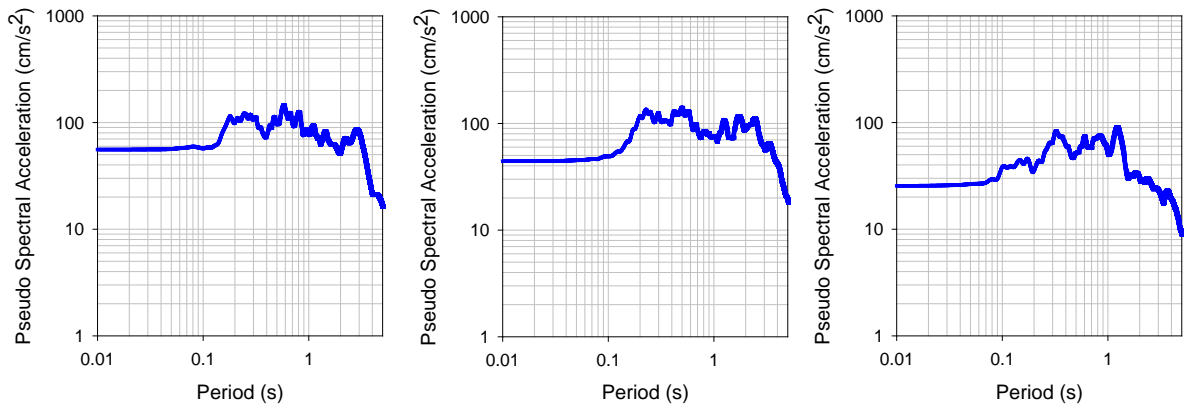


Figure A.2. 5% damped pseudo-spectral accelerations of the processed ground motions recorded at Muş-Malazgirt (Record Name: 20111023104120\_4902, Station Code: 4902).  
 First column: EW component, second column: NS component and third column: UD component.

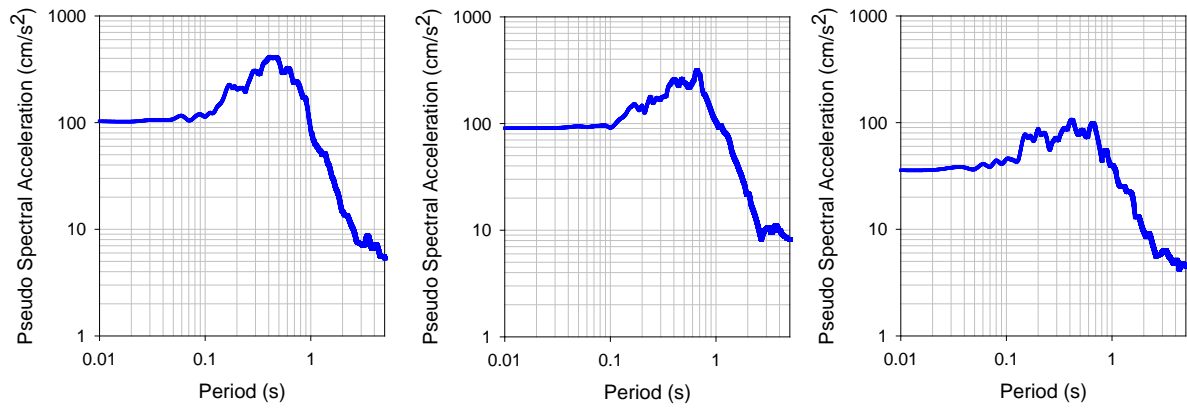


Figure A.3. 5% damped pseudo-spectral accelerations of the processed ground motions recorded at Bitlis-Merkez (Record Name: 20111023104118\_1302, Station Code: 1302). First column: EW component, second column: NS component and third column: UD component.

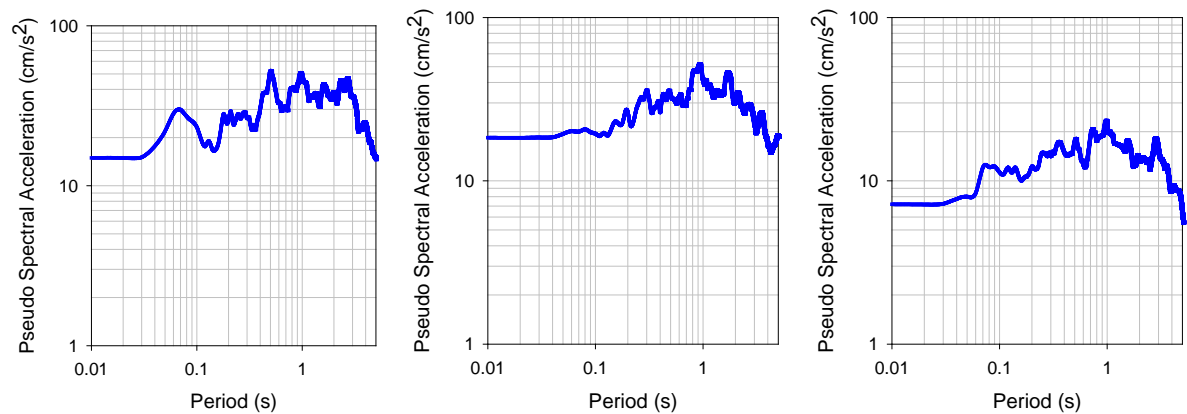


Figure A.4. 5% damped pseudo-spectral accelerations of the processed ground motions recorded at Ağrı-Merkez (Record Name: 20111023104043\_0401, Station Code: 0401). First column: EW component, second column: NS component and third column: UD component.

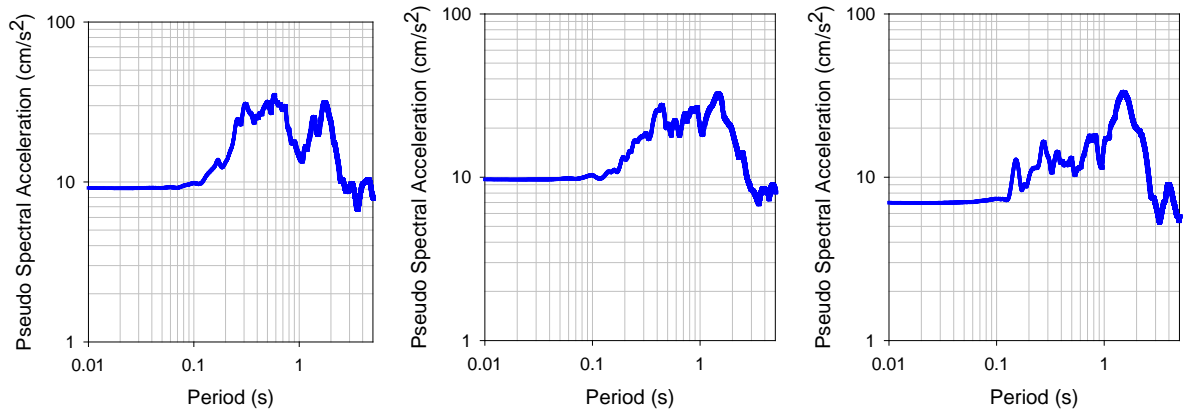


Figure A.5. 5% damped pseudo-spectral accelerations of the processed ground motions recorded at Siir-Merkez (Record Name: 20111023104121\_5601, Station Code: 5601). First column: EW component, second column: NS component and third column: UD component.

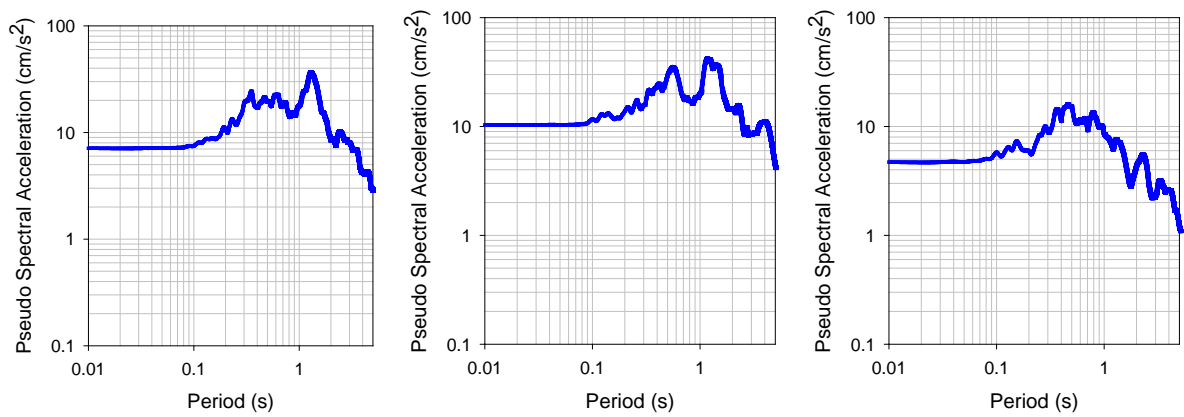


Figure A.6. 5% damped pseudo-spectral accelerations of the processed ground motions recorded at Muş-Merkez (Record Name: 20111023104136\_4901, Station Code: 4901). First column: EW component, second column: NS component and third column: UD component.



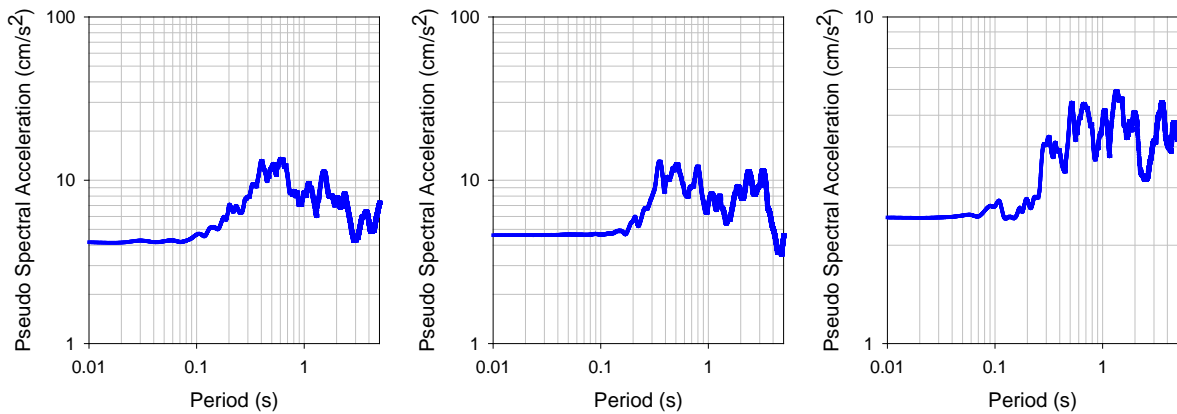


Figure A.7. 5% damped pseudo-spectral accelerations of the processed ground motions recorded at Bingöl-Solhan (Record Name: 20111023104145\_1211, Station Code: 1211).  
 First column: EW component, second column: NS component and third column: UD component.

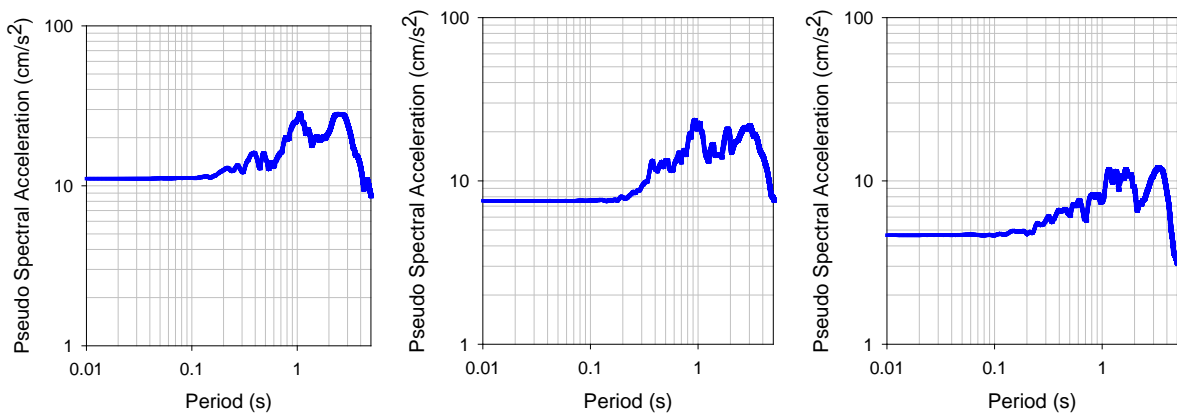


Figure A.8. 5% damped pseudo-spectral accelerations of the processed ground motions recorded at Bingöl-Karlıova (Record Name: 20111023104156\_1206, Station Code: 1206).  
 First column: EW component, second column: NS component and third column: UD component.

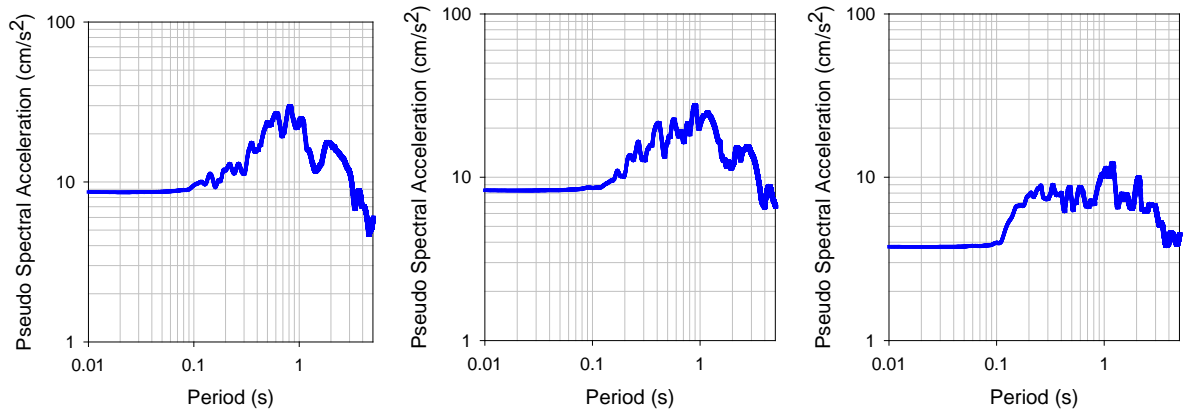


Figure A.9. 5% damped pseudo-spectral accelerations of the processed ground motions recorded at Batman-Merkez (Record Name: 20111023104134\_7201, Station Code: 7201).  
 First column: EW component, second column: NS component and third column: UD component.